Local fracture toughness measurements in polycrystalline cubic zirconia using micro-cantilever bending tests

Ronan Henry, Thierry Blay, Thierry Douillard, Armel Descamps-Mandine, Isabelle Zacharie-Aubrun, Jean-Marie Gatt, Cyril Langlois, Sylvain Meille

Local fracture toughness measurements in polycrystalline cubic zirconia using micro-cantilever bending tests

Ronan Henry [a,b], Thierry Blay [b], Thierry Douillard [a], Armel Descamps-Mandine [c], Isabelle Zacharie-Aubrun [b], Jean-Marie Gatt [b], Cyril Langlois [a], Sylvain Meille *[a]

[a] *Université de Lyon, INSA Lyon, MATEIS UMR CNRS 5510, 7 avenue Jean Capelle, Villeurbanne 69621, France*

[b] *CEA, DEN, DEC, St. Paul Lez Durance 13108, France*

[c] *Centre de Microcaractérisation Raimond CASTAING, Université de Toulouse, CNRS, UT3 – Paul Sabatier, INP, INSA, Espace Clément Ader, 3 rue Caroline Aigle, 31400 TOULOUSE France*

** Corresponding author, sylvain.meille@insa-lyon.fr*

Declarations of interest: none

Abstract

Local fracture toughness of a polycristalline ceramic was characterized with the micro-cantilever bending method. Beams were milled in single grains of cubic zirconia using a Focused Ion Beam (FIB) microscope. Grains with specific crystallographic orientations were chosen using Electron Backscatter Diffraction (EBSD) measurements to test specific plane families. Notched micro-cantilever beams were loaded up to fracture using a nano-indenter. For fracture toughness evaluation, three different methods were considered: an analytical solution, an isotropic Finite Element Method (FEM) calculation, and an anisotropic FEM model. These three methods gave similar toughness values. A good agreement was found with literature data measured on cubic zirconia single crystals at a macroscopic scale. In this work, no significant difference was noticed for fracture toughness between {100}, {110} and {111} crystallographic plane families. Such method could be used to characterize the local fracture properties of a sample showing extensive cracking such as irradiated nuclear fuel.

Keywords

Micro-cantilever testing; Focused ion beam; Fracture toughness; Zirconia

1. Introduction

Nuclear fuel of pressurized water reactor is mainly uranium dioxide UO_2 shaped into cylindrical pellets and inserted in a zirconium alloy cladding. UO_2 is a refractory ceramic that exhibits a brittle behavior in tension up to 900 °C [1]. As the heat produced in a fuel pellet during service is transferred to the coolant by thermal conduction through its periphery, there is a substantial difference in temperature between the pellet center (typically 1000 °C) and its rim (typically 500 °C). Consequently, the periphery expands less than the center and is loaded in tension, leading to a systematic cracking of the fuel pellet at the first power rise. The ceramic crack network evolves in the power reactor during normal operations, power transients, and simulated accident conditions. To better predict the thermo-mechanical fuel behavior in all these conditions, it is necessary to characterize the fracture properties of the fuel material and their evolution with irradiation to feed fuel performance models. In numerical simulations, the two key parameters describing the brittle fracture are the fracture stress and the fracture toughness [2]. These two properties have already been measured on fresh fuel (before irradiation), using macroscopic methods such as bending tests or indentation tests leading to crack propagation after removal of the indentation tip [3]–[5]. However, because of the microstructural transformations induced by irradiation, it is impossible to manufacture macroscopic specimens for mechanical testing into irradiated UO_2 [6]. As a consequence, fracture toughness of nuclear fuel after irradiation has only been assessed by indentation techniques [7][8]. However, the use of Vickers Indentation Fracture toughness tests (VIF) is still debated because of the validity of the hypothesis needed to determine the toughness [9][10].

The aim of this work is therefore to set up an alternative methodology for the local measurement of fracture properties in irradiated nuclear fuel.

Micro- or nano-indentation is no longer the only micromechanics test available for the measurement of fracture properties at a local scale. For example, micro-cantilever bending tests on a ceramic material were first carried out in 1988 by lithographic methods on silicon [11], but this process uses selective etching to mill cantilevers, and is not applicable to most of ceramics. Di Maio et *al.* [12] have extended the applicability of the method using a Focused Ion Beam (FIB) microscope. More recently, Jaya et *al.* [13] reviewed experimental methods for fracture toughness determination using FIB specimens milled in silicon. From literature, the most versatile method for the examination of irradiated nuclear fuel appears to be the single cantilever bending, with a pentagonal cantilever beam section. This geometry is known to give results close to rectangular beam sections [14], and is more convenient to mill, mainly because it can be prepared at any position on the sample surface.

Micro-cantilever bending tests enable the determination of mechanical properties at a local scale, and are particularly adapted for small structures as thin films [15], [16]. These tests can give access to different properties: Young's modulus, fracture stress, or fracture toughness, this last property being measured with a notched cantilever. In this latter configuration, FIB milling can particularly affect the material around the notch because of ion implantation, and thus modify the measured properties. Moreover, local testing in a polycrystalline material with a grain size of a few micrometers can also arise some questions about the influence of microstructure features, as grain boundaries [17], crystallographic planes [17] or anisotropic elastic behavior [18] on the measured properties.

In this paper, we study the ability of notched micro-cantilever bending tests to provide local fracture toughness measurements in a polycristalline ceramic. As irradiated nuclear fuel needs a specific testing environment (nuclearized FIB and indenter), it was chosen to work first on a model material for nuclear fuel, cubic zirconia, with standard testing conditions. This latter method was selected as a model material for UO_2 fuel [19] because it is also a brittle ceramic at room temperature, with:

- Same crystallographic structure ($Fm\bar{3}m$) as UO_2.
- Elastic properties similar to fresh UO_2 fuel (macroscopic values and anisotropic moduli of the crystal).
- Grain size similar to UO_2 fuel (around 10 µm).
- Known fracture properties for polycrystalline and monocrystalline zirconia.

Micro-cantilever beams can have dimensions close to the grain size, so it is possible to work in selected crystallographic planes. Micro-cantilever tests were already carried out in selected crystallographic orientations on single crystals [20]–[22], or in a selected phase in composites or specific grains in a polycrystalline samples [14], [23], but not in selected grains with chosen crystallographic orientations in a polycrystalline material. Fracture toughness values of cubic zirconia in this latter configuration are presented hereafter and discussed in comparison with macroscopic values found in literature on single- and poly-crystals.

2. Experimental details

2.1. Material and preparation

The tested material was 8Y-FSZ zirconia, fully stabilized in cubic phase with 8 mol% of Y_2O_3 (Microcertec, Collegien, France). The sample was a pellet of 8 mm in diameter and 2 mm in thickness. The surface was mechanically polished with diamond suspensions down to 1 µm, and the final preparation step was done with a vibratory polishing using colloidal silica (particle size of 0.03 µm). Finally, in order to avoid specimen charging when using a Scanning Electron Microscope (SEM) or a FIB, a carbon layer of approximately 10 nm was deposited on the surface. The grain size distribution was measured with the software HKL Channel5 (Oxford Instruments, Abingdon-on-Thames, UK) on almost 500 grains by analysis of Electron Backscatter Diffraction (EBSD) maps, leading to an average equivalent diameter of 6.5 ± 3.1 µm. The porosity fraction, measured on backscattered electron imaging in a SEM, was 2.1 ± 0.5 %.

2.2. Crystallographic orientation of cantilevers

EBSD maps were acquired using a Nordlysll fast camera and Aztec software (Oxford Instruments, Abingdon-on-Thames, UK) in a SEM Supra55VP (Carl Zeiss, Oberkochen, Germany). Acquisition was performed with an accelerating voltage of 20 kV, a step of 1.5 µm and a pixel binning of 2x2, leading to an indexation rate around 93%. At this accelerating voltage, EBSD maps can be acquired through the carbon layer. Large grains with an apparent diameter of at least 12 µm, sufficient to include a whole cantilever, were selected (*Figure 1a*). From the crystallographic orientation of grains (*Figure 1b*), it was possible to find and select a grain with a specific plane normal to the surface (*Figure 1c*). Then, a cantilever with a notch oriented along this chosen crystallographic plane was milled (*Figure 1d*).

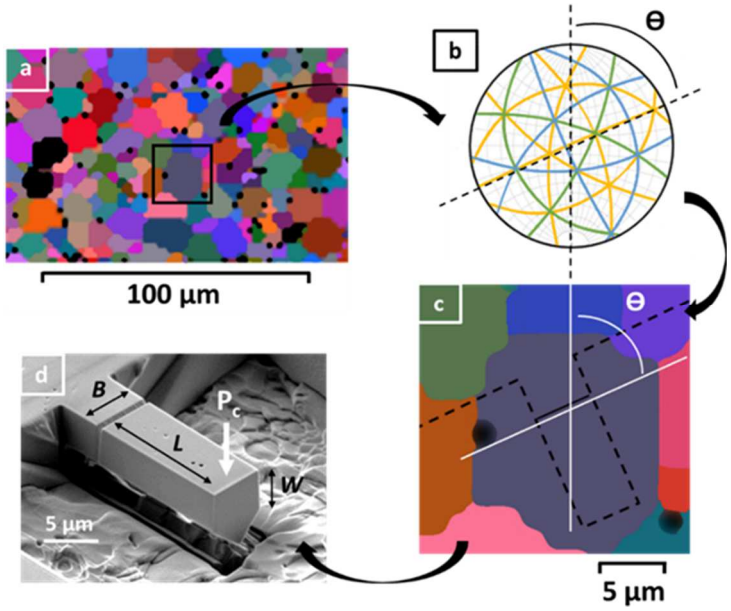

Figure 1 : (a) Example of EBSD orientation map on cubic zirconia, corrected from noise and non-indexed pixels with Kuwahara filters; porosity appears as black pixels. (b) Stereographic projection in the SEM reference frame of the crystallographic planes corresponding to the grain surrounded with a black square in (a). Crystallographic plane families {100} {110} and {111} are represented, respectively, with green, yellow and blue lines. In this orientation, a {110} plane is perpendicular to the surface. (c) Schematic of the future cantilever contour with a notch position parallel to this {110} plane. The crystallographic orientation of the cantilever is fully determined by the combination of three Euler angles from EBSD measurements and of the angular position Θ of the targeted crystallographic plane. (d) Micro-cantilever obtained after FIB milling.

2.3. FIB fabrication

Micro-cantilever beams were milled with a FIB NVision40 at 30 kV (Carl Zeiss, Oberkochen, Germany). When a grain with a suitable crystallographic orientation was selected (Figure 1*a* and Figure 1*b*), a notch was firstly milled along this targeted plane (Figure 1*c*). The ion beam was perpendicular to the sample surface and a low milling current of 10 pA was used to minimize the notch tip radius. The notch was milled first in order to avoid any over-milling effect on the edges of cantilevers [14]. Then, the coarse U-shape contour of the cantilever beam was milled using a 6 nA current, inside a single grain (Figure 1*c*). Undercuts were made with a current of 2 nA after a sample tilt of 54°. In order to correct milling effect of the gallium beam V-shape, every surface was reworked with an over-tilt angle of 2° and a current of 300 pA. The front surface was polished with a current of 80 pA because this surface was used for dimensions measurements. Finally, the micro-cantilever beam (Figure 1*d*) was tilted up to 54°, in order to measure all its dimensions, applying the suitable tilt correcting factor. For the notch depth *a*, the measurement were made after fracture of the cantilever.

2.4. Mechanical tests

Bending tests were performed *ex situ* with a nanoindenter G200 (Keysight Technologies, Santa Rosa, USA). To limit manipulations of samples, a special sample holder was manufactured, adapted for both SEM/FIB and nanoindenter. A Berkovich tip was used, with a force controlled mode at 0.05 mN/s. In order to ease the

positioning of the loading point, target marks were made on the specimens by low current FIB milling. Several tests were also conducted with a nanoindenter PI 85L SEM (Hysitron, Eden Prairie, Minnesota, USA) inside the chamber of a SEM Nova NanoSEM 450 (FEI, Hillsboro, Oregon, USA), using a displacement controlled mode of 5 nm/s. Here, for a better visibility of the loading point with the SEM, the tip used was a Cube Corner.

For every bending test, the load-displacement curve showed a clear load drop at the specimen fracture. This allowed the precise measurement of the fracture load P_c.

3. Fracture toughness calculation

3.1. Analytical method

Fracture toughness can be calculated with an analytical solution, using equation (1) where σ_c is the fracture stress, a is the notch depth, z is the vertical distance between the upper surface and the gravity center G of the cross-section (Figure 2), and $\alpha(a/2z)$ is the shape factor.

$$K_{Ic} = \sigma_c . \sqrt{\pi . a} . \alpha(\frac{a}{2z}) \quad (1)$$

The fracture stress σ_c of a pentagonal cantilever beam is given by equation (2), P_c being the fracture load, L the distance between the notch and the loading point (Figure 1*d*) and I_G the moment of inertia.

$$\sigma_c = \frac{P_c . L . z}{I_G} \quad (2)$$

z can be calculated with equation (3), and I_G with equation (4), using beam dimensions as illustrated in *Figure 2*.

$$z = \frac{3.W^2 + C^2 + 3.C.W}{6.W + 3.C} \quad (3)$$

$$I_G = \frac{B.W^3}{12} + B.W\left(z - \frac{W}{2}\right)^2 + \frac{B.C^3}{36} + \frac{B}{2}.C\left((W - z) + \left(\frac{C}{3}\right)\right)^2 \quad (4)$$

Finally the shape factor $\alpha(a/2z)$ was determined with equation (5), taken from literature [23]. It was initially calculated by a finite element simulation for a given sample geometry, using a *J*-integral analysis, with an elastic and isotropic constitutive law.

$$\alpha\left(\frac{a}{2z}\right) = 0{,}974 + 0{,}242\left(\frac{a}{2z}\right) - 0{,}630\left(\frac{a}{2z}\right)^2 + 3.710\left(\frac{a}{2z}\right)^3 \quad (5)$$

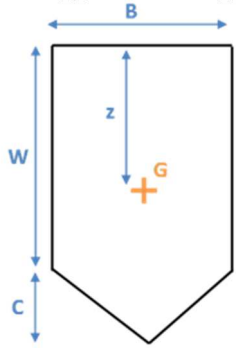

Figure 2 : Sketch of the pentagonal section of a cantilever beam with associated dimensions. G is the gravity center of the section.

3.2. Isotropic Finite Element Method (FEM)

The above analytical solution has been determined for ideal boundary conditions and a perfect sample geometry. To take into account the cantilever support and the actual dimensions of each specimen, a FEM model was used to determine fracture parameters. The critical energy release rate G_c can be calculated with equation (6), depending on the fracture load P_c and on the derivative of the sample compliance C with respect to the crack length a, B being the width of the micro-cantilever beam.

$$G_C = \frac{{P_c}^2}{2B} . \frac{dC}{da} \quad (6)$$

The system was modeled by finite element analysis, using Cast3m Software (CEA, Paris, France), with an elastic constitutive law. To properly represent the limit conditions at the cantilever base, the model includes the cantilever beam and its supporting material. Fixed displacement conditions were applied to the four faces representing the bulk material as illustrated in *Figure 3*. A mesh optimization evidenced the need to reduce the size of elements close to the notch. The notch was considered as a perfect crack here, with unleashed nodes. The load P_c was applied at the cantilever end, at a distance L from its base as measured with the SEM (Figure 1*d*).

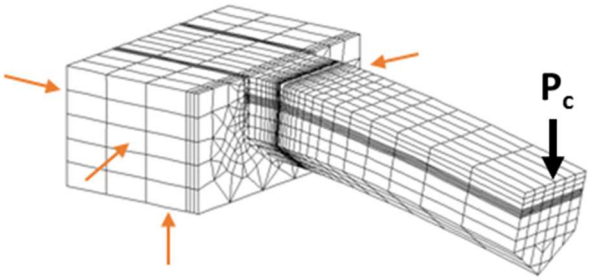

Figure 3 : *Mesh used in FEM simulation of a micro-cantilever bending. For clarity, displacements are amplified here (x5). Orange arrows show faces with a fixed displacement boundary condition.*

In a first step, the system compliance was calculated with the initial notch depth. In a second step, the notch depth a was incremented stepwise by da, and the compliance was again calculated. The difference of these two compliances leads to the term dC/da in equation (6). To calculate the fracture toughness, the isotropic relation between critical energy release rate G_c and fracture toughness K_{Ic} was used (equation (7)), with E' the effective Young's modulus given by $E' = E/(1-\nu^2)$ for plane strain, E the Young's modulus and ν the Poisson ratio.

$$K_{IC} = \sqrt{G_c . E'} \quad (7)$$

As already mentioned by Brinckmann et *al*. [18], there is a difference of crack driving force along the notch, the stress intensity factor being greater at the beam center (plane strain). In this work, plane strain calculation was used, giving the maximum value of the stress intensity factor along the notch. The isotropic Young modulus of 216 GPa and the Poisson's ratio of 0.30 were measured experimentally on a macroscopic polycrystalline sample of cubic zirconia by ultrasonic methods.

3.3. Anisotropic Finite Element Method (FEM)

As each micro-cantilever was machined into a single grain of an anisotropic crystalline material, the influence of elastic anisotropy on the calculation of the toughness should be considered. The same mesh and calculation procedure as for the isotropic case were used, the equation (6) being valid in an anisotropic case [24][25]. Orthotropic elastic properties of cubic zirconia single crystal were entered into the software (C_{11} = 402 GPa, C_{12} = 95 GPa, C_{44} = 56 GPa, giving a Zener's anisotropy ratio of 0.36 [26]). Then, the orthotropic orientation of the beam was provided thanks to EBSD measurements.

The calculation of fracture toughness in an anisotropic case is given by (8) [25][27]:

$$G_I = K_I^2 . \sqrt{\frac{b_{11}.b_{22}}{2}} . \left(\sqrt{\frac{b_{22}}{b_{11}}} + \frac{2.b_{12}.b_{66}}{2.b_{11}} \right)^{\frac{1}{2}} \quad (8)$$

where:

$$b_{11} = \frac{a_{11}a_{33} - a_{13}^2}{a_{33}} , b_{22} = \frac{a_{22}a_{33} - a_{23}^2}{a_{33}} , b_{12} = \frac{a_{12}a_{33} - a_{13}a_{23}}{a_{33}} , b_{66} = \frac{a_{66}a_{33} - a_{36}^2}{a_{33}}$$

in plane strain, we have:

$$a_{11} = \frac{1}{E_1}, \quad a_{13} = \frac{-\upsilon_{13}}{E_1} = \frac{-\upsilon_{31}}{E_3},$$

$$a_{22} = \frac{1}{E_2}, \quad a_{23} = \frac{-\upsilon_{23}}{E_2} = \frac{-\upsilon_{32}}{E_3},$$

$$a_{33} = \frac{1}{E_3}, \quad a_{12} = \frac{-\upsilon_{12}}{E_1} = \frac{-\upsilon_{21}}{E_2},$$

$$a_{36} = 0, \qquad a_{66} = \frac{1}{G_{12}}$$

where $_1$ corresponds to the longitudinal crack direction, $_2$ to the direction perpendicular to the crack and $_3$ to the transverse crack direction. Each Young modulus E_i, Poisson's ration v_{ij} or shear modulus G_{ij}, depending on i and j directions, was calculated using the compliance matrix after its proper transformation by rotation of three Euler angles measured by EBSD, and of Θ angle determined with stereographic projection (*Figure 1*).

4. Results

4.1. Fracture analysis

Fracture surfaces of every specimen were imaged by SEM (*Figure 4*). The notch made directly on the surface sample during the first milling step presented no over-milling effect on the edges of cantilevers (*Figure 4a*). The fracture surface was always smooth (*Figure 4a*) in every tested planes, suggesting a brittle fracture of cantilevers. The crack path was first straight in the upper part of the cantilever, and then deviated in the lower part (*Figure 4b*). This phenomenon, already known on macroscopic bending samples as "cantilever curl", was described on microscopic beams by Norton et *al.* [17], and is due to compressive stresses in the lower part of the cantilever. Because of this deviation, measurement of the notch depth can be difficult, as the contrast at the notch tip can be confused with the contrast at the changing crack path (*Figure 4c*).

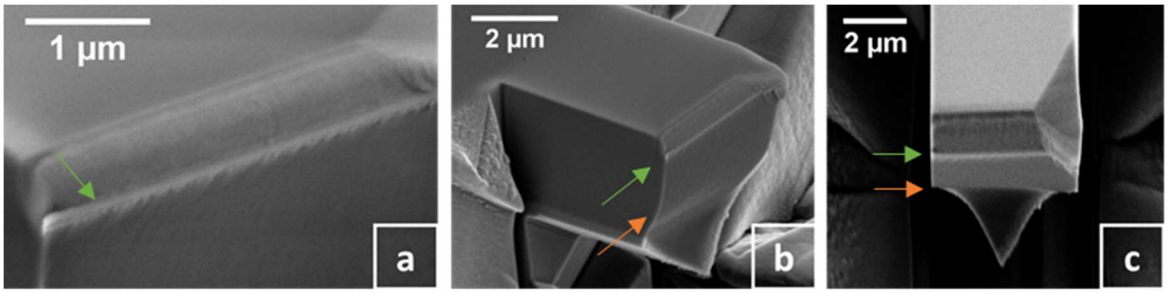

Figure 4 : *(a) SEM fractography from a notched beam after bending test, showing a smooth surface, characteristic of brittle fracture. (b) SEM fractography of the same surface from a different angle. (c) SEM fractography of the same surface, taken frontally, with a tilt angle of 20° and using the proper tilt correction factor. The green arrow shows the notch bottom, the orange arrow shows the crack deviation due to "cantilever curl" effect. The mark on the right of the cantilever is an imprint left, after fracture of the cantilever, by the indenter tip.*

Experimental force-displacement curves needed to be corrected from the tip penetration into the specimen [28]. For every bending test, an indentation was done up to the experimental fracture load of the beam, next to

the micro-cantilever beam. The indentation curve obtained was subtracted to the raw curve in order to obtain the flexion curve (*Figure 5*). Corrected curves showed a linear trend up to fracture for every conducted test obtained either *in situ* with a displacement controlled mode or *ex situ* with a force controlled mode, confirming the linear elastic behavior and the brittle fracture. It was also supported by cyclic tests conducted on notched and un-notched specimens, where successive loading and unloading cycles showed no irreversible deformation after unloading phase.

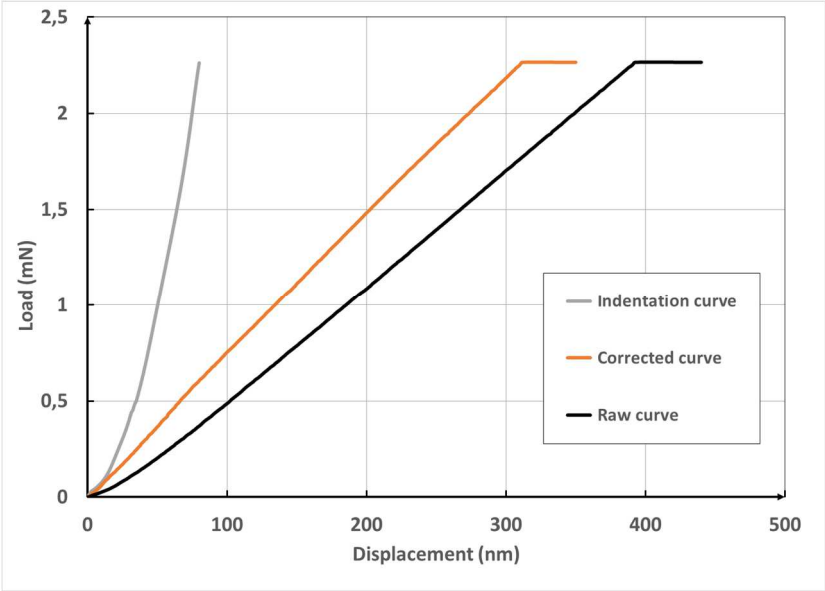

Figure 5 : Typical load-displacement curves obtained during a bending test of a micro-cantilever beam. Raw curve: obtained during the bending test. Indentation curve: conducted next to the micro-cantilever beam up to the fracture load measured on the raw curve. Corrected curve: obtained by subtraction of the displacement of the raw curve by the displacement of the indentation curve.

4.2. Fracture toughness evaluation

Single grains of polycrystalline cubic zirconia were tested. More specifically, loads at failure of micro-cantilevers milled into three families of crystallographic planes {100}, {110} and {111} were measured (*Table 1*).

Table 1 : Fracture load, fracture toughness and dimensions of the cantilevers tested (as illustrated in *Figure 1* and *Figure 2*). Tests marked with * were carried out using a displacement controlled mode of 5 nm/s; tests with no mark were carried out with a force controlled mode of 0.05 mN/s.

Crystallographic orientation	**Specimen number**	**Dimensions (µm)**					**Fracture load (mN)**	**Fracture toughness ($MPa.m^{0,5}$)**
		W	***B***	***C***	***L***	***a***	P_c	**Analytical K_{IC}** (equation (1))
{100}	1	2.98	5.98	2.73	9.20	1.32	1.53	1.44
	2	2.84	4.99	2.41	9.97	0.64	1.63	1.50
	3	3,44	6.27	3.15	9.74	0.70	3.28	1.57
	4	3.38	6.21	2.56	9.10	0.61	2.27	1.14
{110}	5	3.15	4.57	2.11	8.03	0.56	2.29	1.65
	6*	3.18	4.42	2.17	8.76	0.91	1.51	1.56
	7*	2.27	4.40	2.10	12.11	0.64	0.87	1.63
{111}	8	2.93	4.99	2.75	8.76	0.50	2.75	1.68

	9	3.16	5.34	2.82	8.13	0.42	3.68	1.59
	10	3.05	3.45	2.14	7.19	0.84	1.28	1.42
	11	3.52	4.18	2.17	7.33	0.56	2.13	1.29
	12	2.99	4.56	2.29	9.40	0.70	1.46	1.41
	13	3.02	5.25	2.67	7.08	0.83	2.21	1.35
	14*	2.64	3.94	1.72	9.96	0.63	0.82	1.32

Fracture toughness were calculated by the three different methods described previously. Data are presented in *Table 2*. The standard deviation makes the assumption of a Gaussian distribution, and the resulting coefficient of variation is up to 15% of the average value. Uncertainties for measurements here were mainly due to uncertainties of dimension measurements, load uncertainties being negligible, as already noticed by Luo et *al*. [14]. These authors evaluated a relative error due to dimension measurements of 10% of the fracture toughness value. This estimated error is in the range of the standard deviation, and is probably the main source of result scattering in this study.

Table 2 : Fracture toughness results obtained with different calculation methods on different crystallographic planes of cubic zirconia.

	K_{IC} (MPa.m^{0,5}) of tested crystallographic planes		
Calculation method	**{100}**	**{110}**	**{111}**
Analytical	1.41 ± 0.19	1.61 ± 0.05	1.44 ± 0.15
FEM isotropic	1.49 ± 0.13	1.65 ± 0.04	1.45 ± 0.14
FEM anisotropic	1.43 ± 0.09	1.60 ± 0.14	1.52 ± 0.15
Number of specimens	4	3	7

No significant difference of fracture toughness is noticed between the three crystalline orientations tested, even if the elastic anisotropy is taken into account into the calculation (*Table 2*). A Student test on data sets shows with 5% of risk that the fracture toughness measured is not statistically different in each tested family of planes.

4.3. Effect of nanoindentation instrumentation

Bending experiments were conducted with two different nanoindentation systems. The first was *ex situ* of the SEM and uses an optical system with a moving stage, which can lead to uncertainties of position of the tip during the test. The second system was *in situ* of the SEM chamber, and a pre-positioning protocol was used before the bending test: a low load of 0.10 mN was applied in order to control the loading point position, allowing a very accurate positioning. Toughness obtained in both cases gave very close results (Table 2), showing that the *ex situ* system, with the help of FIB positioning marks, gives consistent results.

5. Discussion

5.1. Comparison between calculation methods

Analytical and FEM isotropic methods gave almost the same results, in every crystallographic family of plane tested (Table 2). This shows that the analytical solution gave satisfactory results for the geometries used. Thus, the influence of the non-ideal boundary conditions is low in these configurations, where the distance between the notch and the supporting material is, at least, of 10% of the beam length.

Brinckmann et *al*. [18] studied numerically the influence of elastic anisotropy using a transverse isotropic model, and showed that it can influence the calculated value of K_{IC}. They concluded that, in most of the cases, elastic anisotropy has a limited influence on fracture toughness calculations: for most of materials, the

difference induced by anisotropic calculation as compared with isotropic one is less than 5%. However, the material used in the present work has a cubic structure, so an orthotropic elastic behavior. In order to quantify effects of this anisotropy on the toughness calculation, an orthotropic FEM modelling was used to determine G_c and K_{IC}. Results found by this method do not show significant difference with values found by isotropic methods (Table 2), confirming the conclusion of Brinckmann et *al*. [18], but on a cubic system.

5.2. Data from literature

Fracture properties of fully stabilized cubic zirconia, with Y_2O_3 mol% ranging from 8 to 10%, has been studied at the macroscopic scale. Fracture toughness is well documented for polycrystalline zirconia, and some values are also available for orientated single crystals determined using different test methods. Some of the results available in literature are summarized in *Table* 3.

Fracture toughness measured on polycrystalline cubic zirconia lies around 1.35 MPa.m$^{0.5}$ and 2.0 MPa.m$^{0.5}$ [29]–[32]. The experimental variation is likely related to differences in microstructural characteristics such as porosity fraction and grain size. The average value is close to the fracture toughness measured on single crystals. For oriented single crystals, results available in literature are essentially determined from VIF experiments [33]–[36]. Toughness for {100} planes, lying between 1.3 MPa.m$^{0.5}$ and 1.9 MPa.m$^{0.5}$ [33], [35], [36], seems higher than {110} planes, which lies between 0.84 MPa.m$^{0.5}$ and 1.48 MPa.m$^{0.5}$ [33], [34], [35]. The VIF method is the most convenient for testing crystallographic planes, but presents limitations for determining fracture toughness anisotropy. As explained in [34], the initial analysis of Anstis et *al*. [37] is based on an elastic and isotropic assumption for the material behavior, and could therefore be affected by an anisotropic behavior. Stanescu et *al.* [34] also showed that VIF method gives a higher resistance of the plane {111} as compared to the {110} type. This result does not agree with the well-established fact that in a fluorite type crystal, as cubic zirconia, {111} is the preferred cleavage plane and should have therefore a lower toughness than {110} [34]. Only one reference compared fracture toughness of two crystallographic planes by Single Edged Notched Beam (SENB) [33], with only two tests for each plane, and another test rejected for the {100} planes because of an unusually high toughness. It gave a higher resistance of the {100} planes compared to {110} planes (1.9 MPa.m$^{0.5}$ against 1.48 MPa.m$^{0.5}$). The same authors also compared SENB experiments with VIF experiments [33], and showed that cracks induced by indentation do not necessary lie in the targeted crystallographic plane. Then, they explained that the fracture toughness measured by VIF was over-estimated for {100} planes, and mentioned that the good agreement between SENB and VIF measurements for {100} planes “must have been accidental” [38].

From literature data, fracture toughness of single crystals and polycrystalline cubic zirconia appears to be in the same range. For toughness of crystallographic planes, even if the value of {100} seems slightly higher than the fracture toughness of {110}, more data are needed to conclude. Indeed, VIF seems not well adapted to the measurement of anisotropic crack propagation resistance, and only very few samples were tested by SENB.

Table 3 : Fracture toughness of fully stabilized cubic zirconia measured by different macroscopic methods from literature. VIF is Vickers Indentation fracture Toughness test, SENB is Single Edge Notched Beam, and DCB is Double Cantilever Beam. Samples are either polycrystalline or monocrystalline.

		Macroscopic K_{IC} (MPa.m^{0,5}) of dense cubic zirconia (8 and 10 Y-TZP) and orientation			
Ref.	**Method**	**{100}**	**{110}**	**{111}**	**Polycrystalline**
[33]	*SENB*	1.9 ± 0.1	1.48 ± 0.04		
[33]	*VIF*	1.9 ± 0.1	1.1 ± 0.1		
[35]	*VIF*	1.3	0.84		
[34]	*VIF*		1.1 ± 0.05	1.48 ± 0.07	
[36]	*VIF*	1.8 ± 0.5			
[29]	*SENB*				1.54 ± 0.05
[30]	*SENB*				2.00 ± 0.1
[31]	*VIF*				1.5
[32]	*DCB*				1.35 ± 0.15

5.3. Comparison between this study and literature

In this work, the same method for toughness determination was applied on {100}, {110} and {111} planes of cubic zirconia. It is possible to compare the results as the milling process of beams and notches was the same for each orientation. Fracture toughness obtained by micro-cantilever bending tests on single grains in this work (*Table 2*) are in the range of macroscopic values found in literature (*Table 3*), with an average fracture toughness around 1.5 MPa.m$^{0.5}$. For fracture toughness along different planes, literature gives a range of values of 1.3-1.9 MPa.m$^{0.5}$ for {100} plane, 0.84-1.4 MPa.m$^{0.5}$ for {110} plane and 1.48 MPa.m$^{0.5}$ for {111} plane. In the present work, results are in good agreement with literature, with 1.41 ± 0.19 MPa.m$^{0.5}$, 1.61 ± 0.05 MPa.m$^{0.5}$ and 1.44 ± 0.15 MPa.m$^{0.5}$, for {100}, {110} and {111} planes respectively.

Toughness measured for {110} plane is slightly higher than the other tested planes in this study, whereas according to literature, this plane seems less resistant than {100}. The influence of the crystalline orientation on the fracture toughness measures is discussed more in details hereafter.

5.4. Influence of crystallographic positioning

A potential issue is that the tested plane could be not perfectly perpendicular to the axis of cantilevers, then the notch would not be perfectly along the targeted plane. This can be due to a combination of several uncertainties. The first comes from the equipment: large EBSD maps were made and tilt movements of the sample were needed to pass from EBSD to FIB configuration, leading to an angular shift estimated between 0.5° and 1°. An uncertainty can also be introduced by using stereographic projections. A plane perpendicular to the surface is selected when represented by a straight line in the graph, passing by the origin. In practice, there is always a possible slight shift of the plane with the targeted orientation, between approximately 0° and 2°, estimated on several stereographic projections. Finally, even if a difference of several degrees between the target plane and the notch plane, the notch should be very close to the targeted orientation. In the case of a cleavage plane, the crack would have probably follow this particular direction. Indeed, crack deflection in notched micro-cantilever bending experiments has already been observed. In monocrystalline alumina [17] and magnesium aluminate spinel [39], a stronger plane leads to a crack deflection toward weaker planes, in which the fracture surface is flat and smooth.

5.5. Effect of notch tip radius

Fracture toughness is known to increase with the notch root radius. Here, an ionic current of 10 pA was used to mill every notch, leading to a thin tip notch radius ρ. The same fabrication process was used for every notch, leading to a similar notch root radius for each micro-cantilever beam. However FIB sputtering yield is known to be driven by crystallographic orientation, and this effect could affect the root radius. However, this phenomenon could not be observed, and the difference of notch root radius between the three crystallographic orientations tested was either inexistent or too small to be characterized with a SEM. Measurements of ρ by FIB/SEM gave a value lying between 10 nm and 20 nm, with no noticeable difference between crystallographic orientations. This result is in the same range of results found by other authors with a milling current of 10 pA : Norton et *al*. [17] measured 15 nm on alumina, and Best. et *al*. [41] found between 15 nm and 25 nm on CrN. It has been shown that a blunt notch leads to an overestimation of fracture toughness [16], [17]. However, for a notch tip radius of less than 20 nm, the error is relatively low, in the range of 10% on alumina [17] and on CrN [16]. The method for fracture toughness correction for notch tip radius introduced by Picard et *al.* [42] was used here to take into account the value of ρ, leading to a correction factor of 0.96. This value was calculated using the fracture stress of cantilevers, determined by bending experiments on un-notched micro-cantilever beams (four specimens), giving a fracture stress of 2.5 ± 0.7 GPa (no information on the crystallographic orientation). Finally, even if the notch tip radius may affect fracture stress measurements, the influence seems to be negligible in this study. The error induced does not exceed 10%, in the range of standard deviation of the experimental measurements. As each micro-cantilever beam was fabricated under the same milling conditions, fracture toughness should be comparable from a crystal plane to another.

5.6. Effect of ion damage

The effect of ionic implantation on fracture toughness measurement is not clear for now. Jaya et *al*. [13] showed that different micro-mechanical tests provide fracture toughness values in good agreement between them, but also with values obtained by other methods. They concluded that, on monocrystalline silicon, there was no significant effect of ion implantation on the measured properties. On the other hand, some authors showed a strong influence of ion implantation on tests carried out on polycrystalline thin film of CrN [16] and on monocrystalline Al_2O_3 [17]. In this last case, the authors explained it by residual stresses induced by the implantation of gallium ions. In the present work, it may lead to an averaging of fracture properties between planes. Moreover, ions are known to “channel” along crystal planes when the sample is favorably orientated, going further into the matter [40]. This phenomena could lead to more and/or deeper implantation in some specific orientations, and thus to a different fracture toughness.

5.7. Chevron notch cantilever

In order to limit ion beam damage effect, a solution could be to work with a perfectly sharp crack (no notch root effect) which had propagated in a non-ion implanted area before complete fracture. To do so, an attractive method was introduced by Mueller et *al*. [43], proposing to use a chevron notch which leads to a stable crack propagation before fracture. The authors showed the efficiency of the method on materials with a homogeneous microstructure through the high of the cantilever: a nano-grained alumina and an amorphous fused silica.

The protocol of fabrication was reproduced here, leading to some difficulties. Actually, to design a chevron notch, more matter has to be removed than for a straight notch. Using a FIB current of 10 pA has led to a non-acceptable shape (Figure 6*a*), at least for a reasonable milling time. Also, chevron notch was made with an ion beam which was not normal to the sample surface. In this configuration, the notch was wider than a straight notch because of the beam conic shape, and using 40 pA has led to a perfect shape but a wide notch (notch root radius of approximately 250 nm, measured by SEM) (Figure 6*b*). Finally a mixed solution was also tried: a pre-notch was done at 40 pA, and then the notch was “sharpened” with a 10 pA current and an over-tilt of 2° (Figure 6*c*).

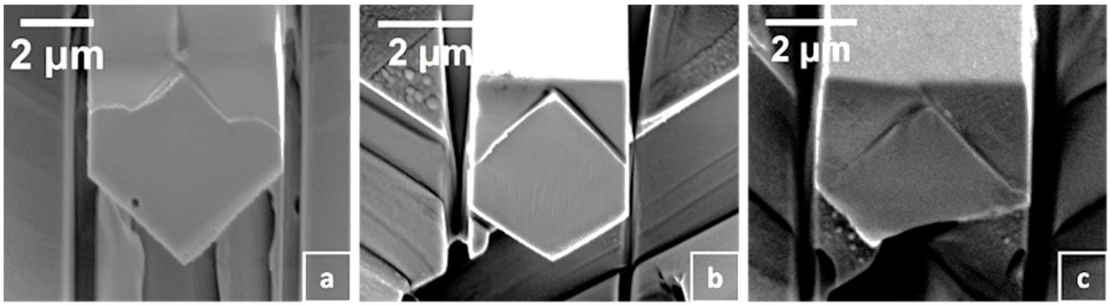

Figure 6 : SEM pictures of micro-cantilever beams with a chevron notch after fracture. (a) Milling current of 10 pA was used: after one hour of milling, the chevron was not completed. (b) 40 pA : the shape was perfect, but the notch was wide. (c) Firstly 40 pA was used, and then 10 pA was used to sharp edges of the chevron.

Whatever the current and the process used to mill the chevron notch, no detection of any stable crack initiation or propagation was possible using the two different nanoindenters. No event in the load-displacement curve or on the fracture surface was noticed. If the calculation is made with the assumption of a stable propagation as described in [43], the fracture toughness measured is highly variable: between 1.06 MPa.m^{0,5} and 2.60 MPa.m^{0,5} on six different tests (another specimen gave an unsually high value of 4.16 MPa.m$^{0.5}$). Chevron-notches were probably too wide, and the stress needed to initiate the crack led to the failure of the whole cantilever. This phenomenon was already noticed by Mueller et *al*. on a single crystal of silicon [24], where the authors mentioned crack initiation issues. The conclusion made in this study is that crack propagation mode of chevron notch is probably material dependant, and for a single-grain of cubic zirconia, the protocol used in the present work has to be modified.

6. Conclusion

The main goal of this methodological work was to study different parameters of the micro-cantilever bending method in order to apply it on fresh and irradiated nuclear fuels. To do so, a model material was used, with properties close to those of UO_2. Thus, notched micro-cantilever bending experiments were conducted on 8mol% of Y_2O_3-fully-stabilized cubic zirconia, leading to the following conclusions:

- The FIB fabrication demonstrated the ability to prepare micro-beams into single grains of a polycrystalline material in specific crystallographic directions. The notching process led to a narrow notch, with a constant depth along the cantilever beam width and no over-milling effect.
- Two different indentation apparatus were tested, *ex situ* and *in situ* in a SEM, leading to similar results on cubic zirconia.
- Fracture surfaces and load-displacement curves confirmed the brittle behavior of the specimens. A change in the crack path at the lower part of the cantilever had to be considered to avoid any confusion in measurement of the notch depth.
- A detailed analysis of bending tests was made using three types of calculation of the fracture toughness: analytical calculation, isotropic and anisotropic FEM calculations. All three methods gave close results.
- Fracture toughness was in good agreement with literature data reported by macroscopic methods, on single crystals or on polycrystalline zirconia of the same composition. Then, it is reasonable to think that ion beam damages have a relatively limited influence on toughness measurements made with a straight notch at 10 pA on this material.
- For the first time, fracture toughness of the three crystallographic families of planes {100} {110} and {111} were measured on cubic zirconia and compared with the same sample, method and equipment. For these three specific families of planes, no significant difference on the toughness results was reported here from a plane to another, which seems to be in contradiction with literature where the {110} planes are slightly weaker than {100} planes. However, only a relatively limited number of conventional SENB tests are available in the literature on cubic zirconia.

- The chevron notch method was tried to quantify ion beam damage effects, but stable crack propagation was not achieved. Results from straight notches are in the range of values of literature, so it is reasonable to assume that ion beam damage effects were low in these experiments.

Finally, the flexure test method of micro-cantilever with a straight notch, studied on cubic zirconia, seems suitable for irradiated nuclear fuel. Even if there are some uncertainties about consequences of ion beam effect on measurements, the method is very attractive for probing fracture properties of the irradiated nuclear fuel.

Acknowledgements

This project is jointly funded by CEA and INSA-Lyon. N. Tarisien and X. Iltis are gratefully thanked for helping in *in situ* experiments. The authors also thank EDF and Framatome for their financial support, and the CLYM (www.clym.fr) for access to microscopes.

References

[1] C. Gandhi and M. F. Ashby, "Overview no. 5. Fracture-mechanism maps for materials which cleave: F.C.C., B.C.C. and H.C.P. metals and ceramics," *Acta Metall.*, vol. 27, no. 10, pp. 1565–1602, 1979.

[2] B. Michel, J. Sercombe, G. Thouvenin, and R. Chatelet, "3D fuel cracking modelling in pellet cladding mechanical interaction," *Eng. Fract. Mech.*, vol. 75, no. 11, pp. 3581–3598, 2008.

[3] A. G. Evans and R. W. Davidge, "The Strenght and Fracture of Stoichoimetric polycristalline UO2," *J. Nucl. Mater.*, vol. 33, no. 33, pp. 249–260, 1969.

[4] H. Matzke, T. Inoue, and R. Warren, "The surface energy of UO2 as determined by hertzian indentation," *J. Nucl. Mater.*, vol. 91, no. 1, pp. 205–220, 1980.

[5] T. R. G. Kutty, K. N. Chandrasekharan, J. P. Panakkal, and J. K. Ghosh, "Fracture toughness and fracture surface energy of sintered uranium dioxide fuel pellets," *J. Mater. Sci. Lett.*, vol. 6, no. 3, pp. 260–262, 1987.

[6] J. M. Gatt, J. Sercombe, I. Aubrun, and J. C. Ménard, "Experimental and numerical study of fracture mechanisms in UO2nuclear fuel," *Eng. Fail. Anal.*, vol. 47, no. PB, pp. 299–311, 2015.

[7] J. Spino, K. Vennix, and M. Coquerelle, "Detailed characterisation of the rim microstructure in PWR fuels in the burn-up range 40-67 GWd/tM," *J. Nucl. Mater.*, vol. 231, no. 3, pp. 179–190, 1996.

[8] K. A. Terrani, M. Balooch, J. R. Burns, and Q. B. Smith, "Young ' s modulus evaluation of high burnup structure in UO2 with nanometer resolution," *J. Nucl. Mater.*, vol. 508, pp. 33–39, 2018.

[9] G. D. Quinn and R. C. Bradt, "On the vickers indentation fracture toughness Test," *J. Am. Ceram. Soc.*, vol. 90, no. 3, pp. 673–680, 2007.

[10] D. B. Marshall *et al.*, "The Compelling Case for Indentation as a Functional Exploratory and Characterization Tool," *J. Am. Ceram. Soc.*, vol. 98, no. 9, pp. 2671–2680, 2015.

[11] S. Johansson, J. Å. Schweitz, L. Tenerz, and J. Tirén, "Fracture testing of silicon microelements in situ in a scanning electron microscope," *J. Appl. Phys.*, vol. 63, no. 10, pp. 4799–4803, 1988.

[12] D. Di Maio and S. G. Roberts, "Measuring fracture toughness of coatings using focused-ion-beam-machined microbeams," *J. Mater. Res.*, vol. 20, no. 02, pp. 299–302, 2005.

[13] B. N. Jaya, C. Kirchlechner, and G. Dehm, "Can microscale fracture tests provide reliable fracture toughness values ? A case study in silicon," *J. Mater. Res.*, vol. 30, no. 5, 2015.

[14] W. Luo, C. Kirchlechner, X. Fang, S. Brinckmann, G. Dehm, and F. Stein, "Influence of composition and crystal structure on the fracture toughness of NbCo2 Laves phase studied by micro-cantilever bending tests," *Mater. Des.*, vol. 145, pp. 116–121, 2018.

[15] K. Matoy *et al.*, “A comparative micro-cantilever study of the mechanical behavior of silicon based passivation films,” *Thin Solid Films*, vol. 518, no. 1, pp. 247–256, 2009.

[16] J. P. Best, J. Zechner, J. M. Wheeler, R. Schoeppner, M. Morstein, and J. Michler, “Small-scale fracture toughness of ceramic thin films: the effects of specimen geometry, ion beam notching and high temperature on chromium nitride toughness evaluation,” *Philos. Mag.*, vol. 96, no. 32–34, pp. 3552–3569, 2016.

[17] A. D. Norton, S. Falco, N. Young, J. Severs, and R. I. Todd, “Microcantilever investigation of fracture toughness and subcritical crack growth on the scale of the microstructure in Al2O3,” *J. Eur. Ceram. Soc.*, vol. 35, no. 16, pp. 4521–4533, 2015.

[18] S. Brinckmann, K. Matoy, C. Kirchlechner, and G. Dehm, “On the influence of microcantilever pre-crack geometries on the apparent fracture toughness of brittle materials,” *Acta Mater.*, vol. 136, pp. 281–287, 2017.

[19] J. Soulacroix, “Approche micromécanique du comportement du combustible dioxyde d’uranium,” *PhD Thesis, ParisTech*, p. 255, 2014.

[20] D. E. J. Armstrong, A. J. Wilkinson, and S. G. Roberts, “Measuring anisotropy in Young’s modulus of copper using microcantilever testing,” *J. Mater. Res.*, vol. 24, no. 11, pp. 3268–3276, 2009.

[21] F. Iqbal, J. Ast, M. Göken, and K. Durst, “In situ micro-cantilever tests to study fracture properties of NiAl single crystals,” *Acta Mater.*, vol. 60, no. 3, pp. 1193–1200, 2012.

[22] B. N. Jaya *et al.*, “Microscale Fracture Behavior of Single Crystal Silicon Beams at Elevated Temperatures,” *Nano Lett.*, vol. 16, no. 12, pp. 7597–7603, 2016.

[23] H. Chan, S. G. Roberts, and J. Gong, “Micro-scale fracture experiments on zirconium hydrides and phase boundaries,” *J. Nucl. Mater.*, vol. 475, pp. 105–112, 2016.

[24] M. G. Mueller, G. Zagar, and A. Mortensen, “Stable room-temperature micron-scale crack growth in single- crystalline silicon,” *J. Mater. Res.*, vol. 32, no. 19, 2017.

[25] T. L. Norman, D. Vashishtht, and D. B. Burr, “Fracture toughness of human bone under tension,” *J. Biomech.*, vol. 28, no. 3, pp. 309–320, 1994.

[26] H. M. Kandil, J. D. Greiner, and J. F. Smith, “Single-Crystal Elastic Constants of Yttria-Stabilized Zirconia in the Range 20° to 700°C,” *J. Am. Ceram. Soc.*, vol. 67, no. 5, pp. 341–346, 1984.

[27] G. C. Sih, P. C. Paris, and G. R. Irwin, “On cracks in rectilinearly anisotropic bodies,” *Int. J. Fract.*, pp. 189–203, 1965.

[28] E. Camposilvan, O. Torrents, and M. Anglada, “Small-scale mechanical behavior of zirconia,” *Acta Mater.*, vol. 80, pp. 239–249, 2014.

[29] R. A. Cutler, J. R. Reynolds, and A. Jones, “Sintering and Characterization of Polycrystalline Monoclinic, Tetragonal, and Cubic Zirconia,” *J. Am. Ceram. Soc.*, vol. 75, no. 8, pp. 2173–2183, 1992.

[30] N. Khan and B. C. H. Steele, “ZrO2-CeO2-Y203 : electrical and mechanical property relationships with the microstructure,” *Mater. Sci. Eng.*, vol. 8, pp. 265–271, 1991.

[31] S. Tekeli, “Influence of alumina addition on grain growth and room temperature mechanical properties of 8YSCZ/Al2O3 composites,” *Compos. Sci. Technol.*, vol. 65, no. 6, pp. 967–972, 2005.

[32] A. N. Kumar and B. F. Sørensen, “Fracture Resistance and Stable Crack-Growth Behavior of 8-mol%-Yttria-Stabilized Zirconia,” *J. Am. Ceram. Soc.*, vol. 83, no. 5, pp. 1199–1206, 2000.

[33] A. Pajares and F. Guiberteau, “Microhardness and Fracture Toughness Anisotropy in Cubic Zirconium Oxide Single Crystals,” *J. Am. Ceram. Soc.*, vol. 71, no. 7, pp. C332–C333, 1988.

[34] J. D. Stanescu and H. M. Chan, “Indentation study of fracture toughness anisotropy in cubic zirconium oxide single crystals,” *J. Mater. Sci. Lett.*, vol. 11, pp. 1364–1365, 1992.

[35] G. N. Morscher, P. Pirouz, and A. H. Heuer, “Temperature Dependence of Hardness in Yttria-Stabilized Zirconia Single Crystals,” *J. Am. Ceram. Soc.*, vol. 74, no. 3, pp. 491–500, 1991.

[36] D. Michel, L. Mazerolles, and M. Perez Y Jorba, “Fracture of metastable tetragonal zirconia crystals,” *J. Mater. Sci.*, vol. 18, no. 9, pp. 2618–2628, 1983.

[37] G. R. Anstis, P. Chantikul, B. R. Lawn, and D. B. Marshall, “A Critical Evaluation of Indentation Techniques for Measuring Fracture Toughness: I, Direct Crack Measurements,” *J. Am. Ceram. Soc.*, vol. 64, no. 9, pp. 533–538, 1981.

[38] A. Pajares, F. Guiberteau, A. Dominguez-rodriguez, and A. H. Heuer, “Indentation-induced cracks and the toughness anisotropy of 9.4-mol%-yttria-stabilized cubi zirconia single crystals,” *J. Am. Ceram. Soc.*, vol. 62, pp. 859–862, 1991.

[39] F. Y. Cui, A. Kundu, A. Krause, M. P. Harmer, and R. P. Vinci, “Acta Materialia Surface energies , segregation , and fracture behavior of magnesium aluminate spinel low-index grain boundary planes,” *Acta Mater.*, vol. 148, pp. 320–329, 2018.

[40] C. A. Volkert, A. M. Minor, and G. Editors, “Focused Ion Beam Micromachining,” *MRS Bull.*, vol. 32, no. May, pp. 389–399, 2007.

[41] J. P. Best *et al.*, “A comparison of three different notching ions for small-scale fracture toughness measurement,” *Scr. Mater.*, vol. 112, pp. 71–74, 2016.

[42] D. Picard, D. Leguillon, and C. Putot, “A method to estimate the influence of the notch-root radius on the fracture toughness measurement of ceramics,” *J. Eur. Ceram. Soc.*, vol. 26, no. 8, pp. 1421–1427, 2006.

[43] M. G. Mueller, V. Pejchal, G. Zagar, A. Singh, M. Cantoni, and A. Mortensen, “Fracture toughness testing of nanocrystalline alumina and fused quartz using chevron-notched microbeams,” *Acta Mater.*, vol. 86, pp. 385–395, 2015.